Measuring single chain dynamics in a polymer melt: from Rouse motion to entanglement distances

An experiment using the Neutron Spin-Echo Spectrometer

School on Methods and Applications of Neutron Spectroscopy
NIST Center for Neutron Research
July 28 – Aug. 1, 2025

Antonio Faraone,[1] Elizabeth Kelley,[1] Michihiro Nagao,[1,2]

[1] NIST Center for Neutron Research, National Institute of Standards and Technology, Gaithersburg, MD, USA

[2] Department of Materials Science and Engineering, University of Maryland, College Park, MD, USA

Abstract

Using neutron spin-echo, we will investigate the nanoscale collective dynamics of long entangling polymer chains in their melt. By means of this experiment, we will illustrate the principles of the neutron spin-echo technique, the required measurements and corrections, and the process of reducing the measured "echoes" to obtain the intermediate scattering function. From the analysis of the intermediate scattering functions, we will examine the Rouse relaxation at short times and obtain the size of the confining tubes in which the chains reptate at longer times.

Table of contents

1. Introduction

1.1. The dawn of the Neutron Spin Echo

Neutron Spin Echo (NSE) spectroscopy is a relatively new technology among neutron scattering techniques. A Hungarian physicist, Ferenc Mezei, first proposed the principle of NSE in 1972 [1]. In the first text book of NSE published in 1980 [2] he described the discovery of the technique as follows: "*The idea of Neutron Spin Echo was born in April 1972 at a red traffic light at the corner of Alagút street in Budapest. Within two weeks the basic points were experimentally verified at the reactor of the Budapest Central Research Institute for Physics. By the end of the year I was also able to demonstrate (this time at the Institut Laue-Langevin in Grenoble) that by this method one can really observe very small velocity changes of a neutron beam, independently of the velocity spread. Soon after, in January 1973, the ILL Council approved the construction of*

a proposed spin echo spectrometer (later to become known as IN11) for high resolution inelastic neutron scattering experiments. ~ by F. Mezei, in preface of Neutron Spin Echo (Lecture Notes in Physics vol. 128)" The key technical concept here is expressed by the specification 'independently of the velocity spread'; this implies that a new method was discovered to perform neutron spectroscopy with unprecedented resolution without sacrificing incoming beam flux, which, in turns, make the measurement practically feasible. Excitement about Mezei's work lead to the rapid development of the first NSE spectrometer in the early 1970s. Nowadays, this technique has been spread worldwide, but is still limited by the number of available instruments (only 2 in the U.S.). Although there are only a few spectrometers in the world, NSE provides new and unique information about dynamics of materials. In this section 1, we introduce some basic concepts about neutron scattering and how we measure dynamics using neutrons.

1.2. Properties of the neutron

Neutrons are non-charged particles (neutron mass m_n=1.67x10^{-27} kg) which display both particle and wavelike nature. A free neutron has momentum $\mathbf{p} = \hbar\mathbf{k}$ and energy $E_p = \left|\frac{\mathbf{p}^2}{2m_\mathrm{n}}\right| = \hbar\omega_n$, where $\mathbf{k}$ and ω_n are the wavevector and frequency, of the associated wave function. $\mathbf{k}$ characterizes the propagation direction and the speed of wave, and the magnitude of $\mathbf{k}$ is $|\mathbf{k}| = k = \frac{2\pi}{\lambda}$, where λ is the wavelength.

Neutrons interact with nuclei during a scattering event. The neutron-nucleus interaction potential V_p is expressed by adopting Fermi's pseudopotential

$$V_p(\boldsymbol{r}) = \frac{2\pi\hbar^2}{m_n} b_i \delta(\boldsymbol{r}) \qquad (1)$$

where $\hbar = \frac{h}{2\pi}$ and h is the Planck's constant, b_i is the so-called neutron scattering length which characterizes the neutron interaction with a given atomic nucleus i, and $\delta(\mathbf{r})$ is delta function and $\boldsymbol{r}$ is the position vector from the scattering center (position of the nucleus i). Different isotopes or spin state of nuclei give different b_i. Since isotopes and nuclear state are randomly distributed in the samples, it is useful to define the coherent, σ_{coh}, and incoherent, σ_{inc}, scattering cross sections as the average and variance of the possible b of a nucleus:

$$\sigma_{coh} = 4\pi\langle b\rangle^2; \sigma_{inc} = 4\pi(b - \langle b\rangle)^2 \qquad (2)$$

where $\langle \ldots \rangle$ indicates an average over all of the possible magnetic nuclear states and isotope compositions. The neutron scattering community frequently uses the difference in the scattering cross sections of different isotopes to tune the scattering length of the materials by the isotope substitution. The values for b_i, σ_{coh}, and σ_{inc} are available at http://www.ncnr.nist.gov/resources/n-lengths/.

Although neutrons are non-charged particles, the internal structure of the neutron allows it to have a magnetic moment. This feature is significant for NSE since we use polarized neutrons, which means one state of the magnetic moment is selected and used in the scattering experiments.

Neutron spectroscopic techniques generally use neutrons that have a kinetic energy that is close to thermal energy, which make neutrons a unique and powerful probe to measure the dynamical features of materials.

Q1:Confirm the energy of neutrons is close to the thermal energy for various wavelengths.

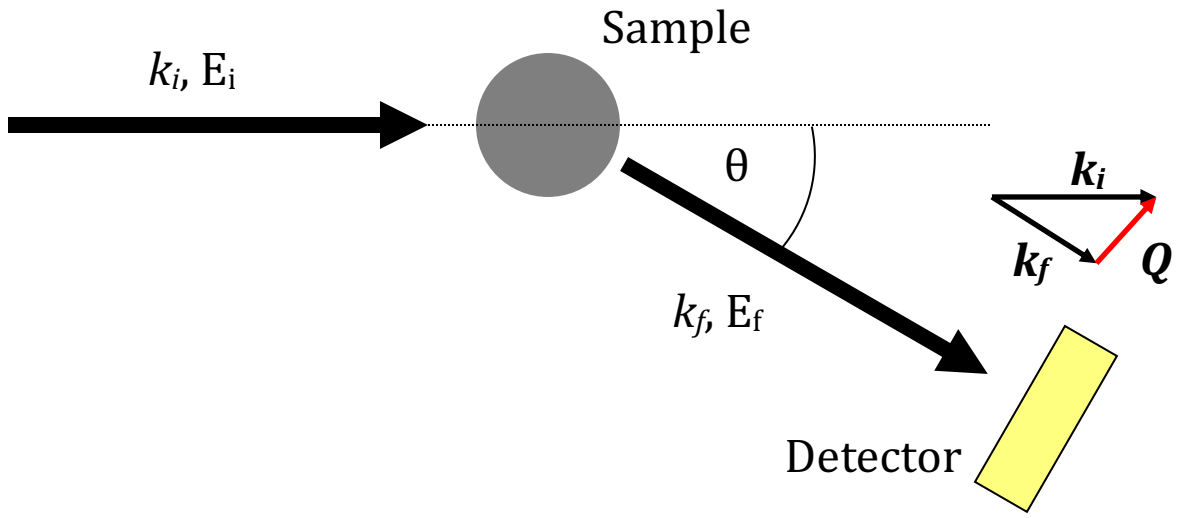

Figure 1. Basic scheme of a scattering experiment.

1.3. Basics of neutron scattering

Consider a neutron beam characterized by its wavevector **k**. If the incoming wave interacts with a nucleus (potential *Vp*) and scatters, the outgoing wave will then have a different wavevector **k'**. Here, we can define the momentum transfer as

$$\hbar\mathbf{Q} = \hbar(\mathbf{k_i} - \mathbf{k_f}) \tag{3}$$

where $\mathbf{Q} = \mathbf{k_i} - \mathbf{k_f}$ is the scattering vector, and the corresponding energy transfer, E, or frequency, ω, is defined as the different energies between incoming, E_i, and outgoing, E_f, wave,

$$E = \hbar\omega = \mathrm{E}_i - \mathrm{E}_f = \frac{\hbar^2}{2m_n}(k_i^2 - k_f^2) \tag{4}$$

Eqns. (3) and (4) describe the momentum and energy conservation of the scattering process, respectively. A basic scheme of a scattering experiment is shown in Figure 1. Here, we consider the magnitude of **Q** by defining the angle between $\mathbf{k_i}$ and $\mathbf{k_f}$ as the scattering angle, θ, and applying $\mathrm{k}_i \approx \mathrm{k}_f$ (*i.e.* small energy transfer) as,

$$|\mathbf{Q}| = Q = 2k\sin\left(\frac{\theta}{2}\right) = \frac{4\pi}{\lambda}\sin\left(\frac{\theta}{2}\right) \tag{5}$$

Using Bragg's law of $2d\sin\left(\frac{\theta}{2}\right) = n\lambda$, where d is the lattice constant and n is an integer, a relationship between Q and a length scale, l, can be roughly established as $Q \approx \frac{2\pi}{l}$. The primary aim of neutron scattering is to determine the probability of neutrons being scattered in **Q** and ω,

which is defined as the dynamic structure factor $S(\mathbf{Q},E)$. The Fourier transform of $S(\mathbf{Q},E)$ is called the Intermediate Scattering Function (ISF), $I(\mathbf{Q},t)$, which is defined as:

$$S(\mathbf{Q},\omega) = FT\{I(\mathbf{Q},t)\} \quad (6)$$

$$I(\mathbf{Q},t) = \langle exp\{-i\mathbf{Q}[\mathbf{r}(t) - \mathbf{r}(0)]\}\rangle \quad (7)$$

where $\langle ... \rangle$ indicates an ensemble average.

In a static structure measurement, we ignore the energy exchange between the neutrons and our samples and integrate the scattering over all neutron energies,

$$S(\mathbf{Q}) = \int_{-\infty}^{\infty} S(\mathbf{Q},E)dE \quad (8)$$

which corresponds to the Fourier transform of the instantaneous spatial atomic correlations in the system, *i.e.* the structure of our sample. In the following discussion, we only consider isotropic scattering cases for simplicity, and treat the vector **Q** as a scalar Q.

1.4. Small-angle scattering

Now let's revisit our definitions of $Q = \frac{4\pi}{\lambda}\sin\left(\frac{\theta}{2}\right) \approx \frac{2\pi}{l}$. If we want to look at large structures (large l), then we need to measure scattering at small Q, which means we need to measure scattering at small angles (small θ). Small angle scattering (SAS) is used to study the structure of materials with sizes ranging from ≈1 nm to ≈200 nm. These length scales are now much larger than the atomic distances, so it is useful to define the scattering length density (SLD), ρ, of a material,

$$\rho = \sum_i^N \frac{b_i}{v} \quad (9)$$

in which v is the volume containing N atoms. In other words, we're averaging the scattering length over the volume of the material. This also means that when we are looking at small Q, we care about the difference in material properties ρ_1 and ρ_2, $\Delta\rho = \rho_1 - \rho_2$, which we refer to as the scattering contrast. It is well-known in the SAS community that one can play tricks with the scattering contrast to make certain parts of our samples appear and disappear in order to highlight specific structural and dynamical features, which is referred to as contrast matching. Among neutron spectroscopic techniques, NSE is the only one whose accessible Q range significantly overlaps with the small angle region, and, hence, is the only one which extensively employs the SLD concepts; other techniques more often deal with atomic scattering lengths and cross-sections.

1.5. Coherent and incoherent scattering

The scattered neutron signal is divided into two components; coherent $S_{\text{coh}}(Q,E)$ and incoherent $S_{\text{incoh}}(Q,E)$ scattering, namely $S(Q,E) = S_{\text{coh}}(Q,E) + S_{\text{incoh}}(Q,E)$. $S_{\text{coh}}(Q,E)$ originates from correlations between relative positions of atoms at different times, and, thus, it contains information about the collective dynamics in our material. In comparison, $S_{\text{incoh}}(Q,E)$ comes from correlations between the positions of an atom at different times, which does not provide any structural information but contains single particle dynamics information. Specifically,

a hydrogen atom has a large incoherent scattering cross section of about 80 barn, and, therefore, it is easy to track the motion of hydrogen atoms via $S_{\mathrm{incoh}}(Q,E)$. It is interesting to note that these two scattering contributions can be distinguished by employing polarization analyses in NSE. Here, we show examples of static structure factors for simplicity, but the basic principle applies for all the scattering events. (See Appendix B for more information about the incoherent scattering and its application to NSE.) Coherent scattering is non-spin-flip scattering (NSF), thus the spin state of neutrons does not change before and after scattering. Overall, there is a 2/3 probability for spin-flip scattering (SF) to occur in incoherent scattering. Using an incoming beam of polarized neutrons (have the same spin state) and a spin analyzer right before the detector that only allows one state of polarized neutrons to pass through to the detector, we can measure the polarization state of the scattered neutrons. A device called π-flipper can then be used to intentionally change the neutron spin state from one to the other. The flipper is turned on to measure the intensity of NSF (N_{up}), and turned off to measure the SF (N_{down}), as

$$N_{\mathrm{up}}(Q) = S_{\mathrm{coh}}(Q) + \frac{1}{3}S_{\mathrm{incoh}}(Q) \tag{10}$$

$$N_{\mathrm{down}}(Q) = \frac{2}{3}S_{\mathrm{incoh}}(Q) \tag{11}$$

Experimentally, care should be taken to measure the instrumental polarization and background scattering to calculate $S_{\mathrm{coh}}(Q)$ and $S_{\mathrm{incoh}}(Q)$.

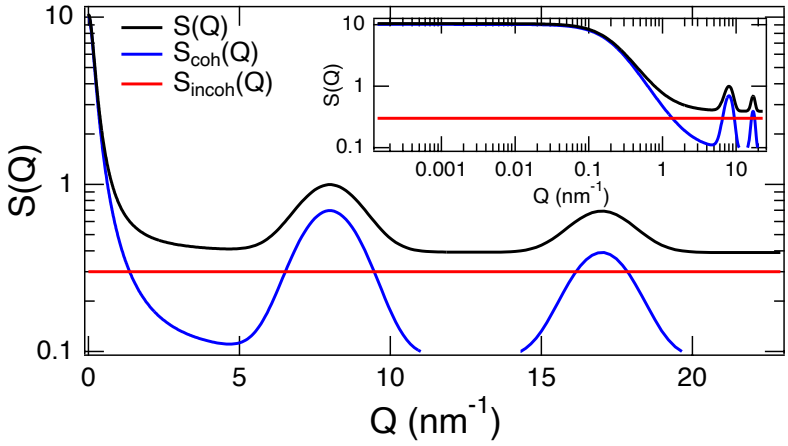

Figure 2. An example of the scattering intensity profile $S(Q)$ together with the characteristics of coherent $S_{\mathrm{coh}}(Q)$ and incoherent $S_{\mathrm{incoh}}(Q)$ signals as a function of Q. The main panel shows the profile in log-linear scale, while inset shows the same profile in log-log scale. Depending on the Q values, the dominant contribution varies between $S_{\mathrm{coh}}(Q)$ and $S_{\mathrm{incoh}}(Q)$.

$S_{\mathrm{coh}}(Q)$ depends strongly on the scattering angle and thus on Q, while in contrast, $S_{\mathrm{incoh}}(Q)$ is independent of Q (for simplicity here we ignore atomic vibrations and the resulting Debye-Waller factor). Figure 2 shows a typical example of a neutron scattering signal $S(Q)$ over a wide Q-range. The inset plots the same scattering pattern on a logarithmic Q scale. At small scattering

angles (small Q), a large $S_{\mathrm{coh}}(Q)$ is recognized due to long range scattering length density fluctuations. The $S_{\mathrm{coh}}(Q)$ decreases with increasing Q, and at some Q-ranges $S_{\mathrm{incoh}}(Q)$ dominates the scattered intensity. Due to structural correlations at smaller length scales, $S_{\mathrm{coh}}(Q)$ might again dominate the intensity at higher Q (for example at $Q \approx 8$ nm^{-1} and 17 nm^{-1} in Figure 2). By varying the isotopic composition of the sample, both coherent and incoherent scattering contributions can be altered.

1.6. Inelastic/quasielastic scattering techniques

The dynamic structure factor $S(Q,\mathrm{E})$ is determined by analyzing the exchanged energy contribution to the scattering at a defined Q. This measurement is called inelastic or quasielastic neutron scattering. Most of the neutron spectrometers determine the incoming and outgoing neutron energies, and their difference corresponds to the energy exchanged. Table 1 summarizes various neutron spectroscopy techniques and their incoming energy and the energy resolution. Since these techniques directly determine the incoming and scattered neutron energies to analyze the energy transfer with the samples, narrow wavelength distribution ($\Delta\lambda/\lambda$) are required in order to achieve higher energy resolution, which limits the number of useful neutrons. Unfortunately, this means that a scattering experiment with high energy resolution would be impossible because of poor counting statistics. As explained below, the NSE technique broke through this limitation, and significantly improved the energy resolution without requiring a narrow $\Delta\lambda/\lambda$.

Table 1. Various neutron spectroscopy and typical parameters.

Technique	Triple-axis spectrometer	Time-of-flight	Backscattering	Neutron spin echo
Instrument	BT7, MACS, SPINS	DCS	HFBS	NGA-NSE
Incoming neutron energy	Variable (*e.g.* 35 meV)	Variable (typically 1 meV to 9 meV)	2.08 meV	0.3 meV to 3 meV
Device to define neutron energy	Monochromator	Chopper	Monochromator	Velocity selector
Neutron wavelength λ	(*e.g.* 1.5Å)	(typically 3 Å to 10 Å)	6.3 Å	5 Å to 15 Å
Wavelength distribution $\Delta\lambda/\lambda$	10^{-3}	Variable	1.86×10^{-5}	0.1 to 0.2
Energy resolution	Variable (*e.g.* 1 meV)	10 μeV to 10 meV	1 μeV	≈ 10 neV

*1 eV corresponds to $1.60\text{x}10^{-19}$ J and to $2.42\text{x}10^{14}$ Hz.

1.7. Characteristics of the NSE technique

Here at the NCNR, the energy resolution for the NGA-NSE spectrometer is ≈ 10 neV, and the best instrument in the world, IN15 in Grenoble, France, is aiming for a few neV. Still the $\Delta\lambda/\lambda$ are of the order of 10%, which gives you enough neutron flux to perform experiments. Figure 3 shows a layout of a NSE instrument. The NSE technique uses polarized neutrons and employs the Larmor precession of the neutron's spin as an 'internal' clock [1]. When the neutron spin direction is parallel to a magnetic field, the polarization of the spin state is kept the same. On the other hand, when the spin is perpendicular to a magnetic field, the spin starts to rotate around the magnetic field (called Larmor precession).

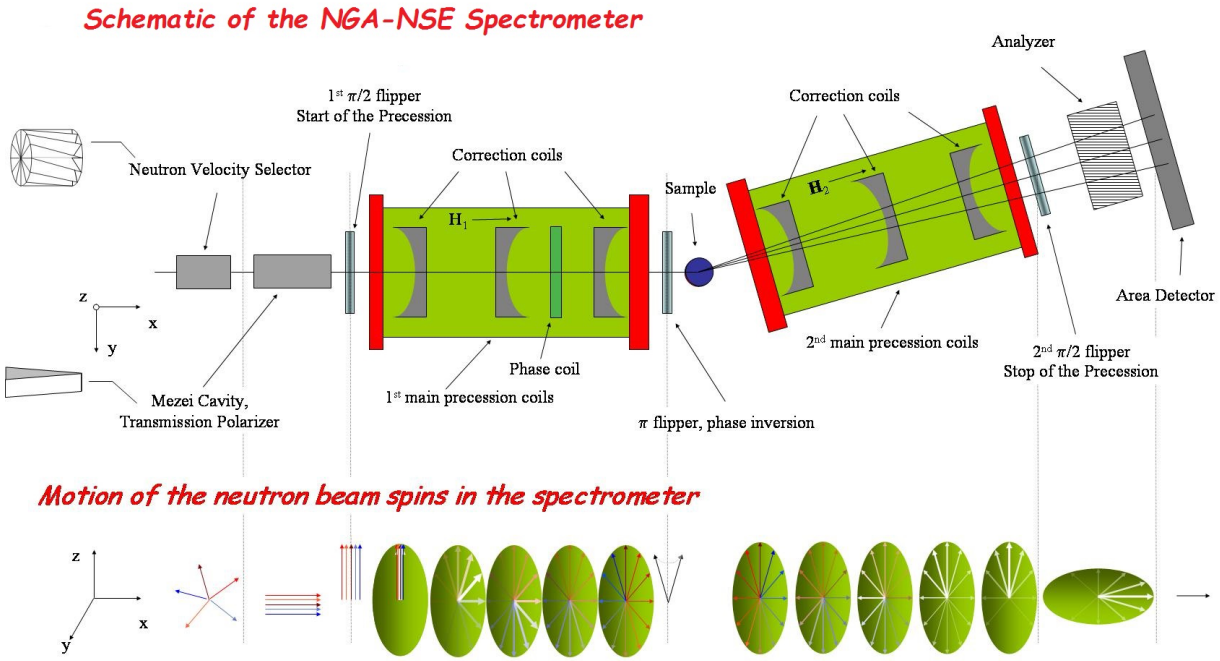

Figure 3. Schematic of the NSE spectrometer and motion of the neutron spins looking perpendicular to the beam direction.

Since the Larmor precession information on the incoming velocity of each neutron is stored on the neutron itself, it can be compared with the outgoing velocity of the same neutron. The basic idea is the following: polarized neutrons are flipped perpendicular to the magnetic field by a so called π/2-flipper. The precession frequency is controlled by a magnetic field along the flight path from the π/2-flipper to the sample. A symmetric setup is placed in the flight path from the sample to a second π/2-flipper. Close to the sample, a π-flipper reverses the precession angle such that for an elastically scattered neutron there is no net spin turn at the second π/2-flipper, irrespective of the starting velocity of the neutron. The precession angles in the primary and secondary paths are

only different when the symmetry is distorted because of a change in the neutron velocity after interacting with the sample. In this case, a polarization change after the second π/2-flipper is observed. Using this set-up, it is possible to make extremely accurate measurements of the energy change during the scattering process, and therefore design a spectrometer with high resolution. Detailed principles of the spectrometer are illustrated in Appendix A.

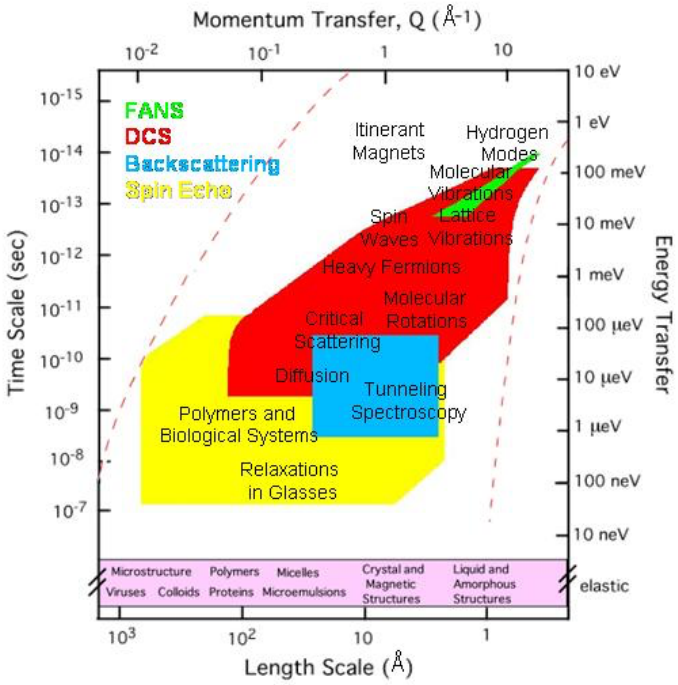

Figure 4. Phase space diagram indicating the regions accessible to the high-resolution spectrometers at the NCNR. Many different fields of application of elastic and inelastic neutron scattering are reported as well.

The reason why we can use relatively broad wavelength distribution and still have a high energy resolution neutron spectroscopy is that the energy resolution of neutron itself (determined by the distribution of velocity V_n or wavelength λ) is decoupled from the energy resolution of the sample's energy transfer that is determined by measuring neutron polarization state in the NSE experiments. This characteristic allows NSE to be the highest energy resolution machine among neutron spectrometers. The use of the NSE technique automatically performs a Fourier transformation in energy and the NSE provide results in the time domain, while all the other neutron spectrometers work in the energy domains. This means that while the conventional neutron spectroscopy measures dynamic structure factor $S(Q,E)$, NSE measures its Fourier transform, the intermediate scattering function, $I(Q,t)$. Because of this unique character, NSE is best suited to measure relaxation processes rather than excitation processes.

1.8. Dynamic range of neutron spectroscopy

Figure 4 summarizes the phase space diagram of neutron spectrometers. Among neutron spectrometers, the NSE covers the smallest Q (largest length scales) and energy scales (highest energy resolution and longest times). Since the coverage of the phase space is at relatively large scale and long time scales, this spectrometer is suited for the investigation of thermal fluctuations in polymer or biological systems. It allows us to investigate length scale up to tens of nanometers and relaxation times from a fraction of a nanosecond to three hundred nanoseconds.

2. Dynamics of polymers [3]

Dynamic processes in polymers occur over a wide range of length and time scales. A typical example is shown in Figure 5. At the local scale, motions like vibrations, short range rotations or secondary relaxation are possible. At temperatures above the glass transition temperature, T_g, the primary relaxation (α-relaxation) originated by the interchain dynamics becomes active. Over larger length scales, conformational dynamics within a polymer chain take place but are limited by confinement effects caused by the mutually interpenetrating chains. This latter dynamic process is responsible for the "rubbery" rheological behavior of polymers. The longest relaxation process is the translational diffusion of the chain. Depending on the molecular weight, the characteristic length scales from the motion of a single bond to the overall chain diffusion may cover about three orders of magnitude, while the associated time scales easily may be stretched over ten or more orders of magnitude. Different neutron scattering techniques can be used to obtain information on these dynamical processes.

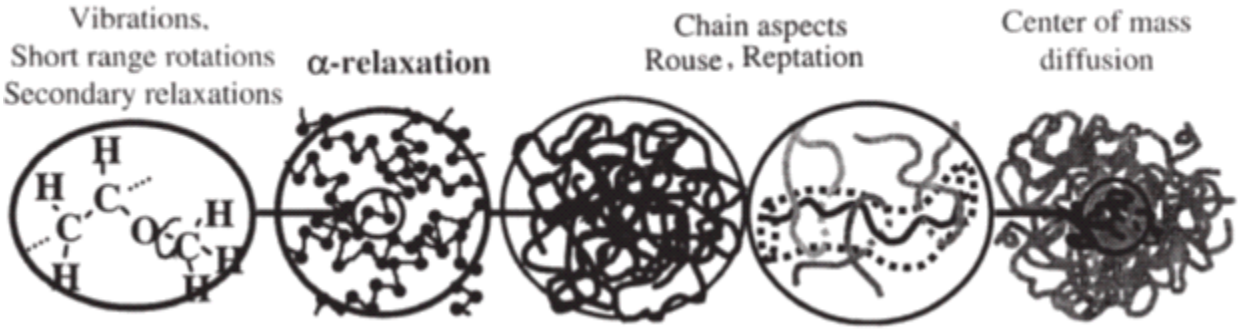

Figure 5. Hierarchical nature of dynamic processes in polymers (adapted from [3]).

Among the experimental techniques for studying the dynamics of polymers, neutron spin-echo spectroscopy plays a unique role because of mainly two reasons:

i. The suitability of the length and time scales, which allows the exploration of large scale properties (*e.g.* diffusion and Rouse dynamics) as well as features characteristic for more local scales (*e.g.* the inter- and intrachain correlations)
ii. The possibility to use isotopic substitution and contrast matching techniques which allows specific structural units or molecular groups in complex systems to be selectively studied.

During this NSE workshop, we will focus on the mesoscale polymer chain dynamics, namely the Rouse and reptation dynamics (see Figure 5), that can be measured using NSE. Recent NSE investigations on the long time chain dynamics confirmed de Gennes' prediction [4] on the mechanism of tube-like confinement and reptation in polymer melts and dense systems. [5] Here, we will perform a similar NSE experiment and measure the ISF of a single polymer chain in a melt as described in detail in the next sections. These measurements will allow us to determine the parameters describing the conformational dynamics of the chains and their entanglements. These results will be compared with literature values obtained using rheological measurements.

2.1. Structure of linear homopolymers

The unique power of neutron scattering for revealing essential features in the field of polymer science can be exemplified by the experimental proof, using Small Angle Neutron Scattering (SANS), of the random coil conformation of polymer chains in the melt or in the glassy state, as proposed in the 1950s by Flory, [6] which was only possible by using contrast variation. In general, flexible long chain polymers possess a very large number of internal degrees of freedom. At length scales somewhat larger than the size of the monomer the detailed chemical structure of the chain building blocks is not important so that very general properties are determined by statistical mechanics of the chain. According to the central limit theorem the most probable arrangement is that of a Gaussian coil, *i.e*. the polymer chain performs a random walk in space. From these assumptions, the form factor for the single chain, which can be measured by SANS, is predicted:

$$I(Q) = f_{Debye}\left(Q^2 R_g^2\right) = \frac{1}{Q^4 R_g^4}\left[exp\left(-Q^2 R_g^2\right) - 1 + Q^2 R_g^2\right] \qquad (12)$$

with R_g being the radius of gyration.

2.2. Rouse dynamics

If pieces of a chain perform fluctuations out of equilibrium, an entropic force arising from the derivative of the free energy acts on these segments to restore them to the most probable contorted state. This is the basis of the so-called Rouse model, [7] and the simplest picture of the model is shown in Figure 6 as a chain of beads connected by springs. The ISF for both single particle dynamics and the collective single chain dynamics can be theoretically predicted and directly measured through opportune deuteration schemes in the incoherent and coherent neutron scattering signal.

2.2.1. Incoherent scattering

The single particle ISF can be measured using hydrogenated samples and measuring the incoherent dynamics. The motion of each hydrogen atom in the chain is described as follows:

$$I_{self}(Q,t) = \langle \sum_{i=1}^{N} exp\{-iQ[\mathbf{r}_i(t) - \mathbf{r}_i(0)]\}\rangle = exp[-Q^2 D_R t] exp\left\{-\left[\frac{t}{\tau_{self}(Q)}\right]^{1/2}\right\} \qquad (13)$$

where D_R is the translational diffusion coefficient of the polymer chain: $D_R = \frac{k_B T}{N\zeta_0} = \frac{Wl^4}{3R_E^2}$, with ζ_0 denoting a friction coefficient, k_BT is the thermal energy, l, N, $R_E=Nl^2$, and $W = 3\frac{k_B T}{\zeta_0 l^2}$ being the polymer segment length, the number of segments in the chain, the end-to-end distance, and the elementary Rouse rate, respectively. The other parameter describing the single particle Rouse dynamics is:

$$\tau_{self}(Q) = \frac{9\pi}{Wl^4Q^4} \quad (14)$$

Within the Gaussian approximation the mean squared displacement of the polymer segments results:

$$\langle r^2(t)\rangle = 6D_R t + \frac{1}{6}\sqrt{\left(\frac{9\pi}{Wl^4Q^4}\right)t} \quad (15)$$

As shown by Eq. (15), for short times, before the chain diffusive dynamics can be observed, the mean squared displacement scales with the square root of time.

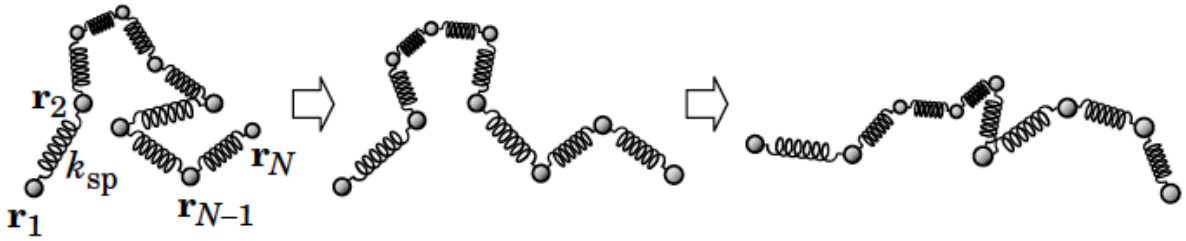

Figure 6. Illustration of chain dynamics in a polymer as the simple bead-spring model that changes its conformation with time. $\mathbf{r}_N$ is the position vector of a bead and k_{sp} is the spring constant (adapted from [8]).

As Q increases, and the investigated length scale gets shorter, local dynamics within the monomer become increasingly important and the Rouse model is not applicable.

The single particle Rouse dynamics of a polymer chain can be measured using NSE as well as other techniques such as backscattering. It is reported here solely to highlight how different spectrometers can be used in conjunction to validate or complement obtained results.

2.2.2. Coherent scattering

Dispersing a small amount of hydrogenated polymer chains in a matrix of deuterated chains, the small angle region will record the coherent signal from the single hydrogenated chains. The single chain dynamics will be measured as the dynamics of one segment with respect to the others:

$$I_{chain}(Q,t) = \langle \sum_{i=1}^{N} exp\{-iQ[\mathbf{r}_i(t) - \mathbf{r}_j(0)]\}\rangle = \frac{1}{N} exp[-Q^2 D_R t]$$
$$\sum_{i,j} exp\left\{-\frac{1}{6}|i-j|Q^2l^2\right\} exp\left\{-\frac{2}{3}\frac{R_E^2Q^2}{\pi^2}\sum_p \frac{1}{p^2}\left\{cos\left(\frac{p\pi i}{N}\right) cos\left(\frac{p\pi j}{N}\right)\left[1 - exp\left(-\frac{tp^2}{t_R}\right)\right]\right\}\right\} \quad (16)$$

Where $t_R = \frac{1}{W}\left(\frac{N}{\pi}\right)^2$ is called the Rouse time. For t=0 we have $I_{chain}(Q,t) = S_{chain}(Q)$; i.e. the structure factor corresponds to a snapshot of the chain structure:

$$S_{chain}(Q) = \langle \sum_{i=1}^{N} exp\{-iQ[\boldsymbol{r}_i(0) - \boldsymbol{r}_j(0)]\}\rangle = \frac{1}{N}\sum_{i,j} exp\left\{-\frac{1}{6}|i-j|Q^2l^2\right\} \quad (17)$$

These predictions have been validated experimentally on short polymer chains. [9]

A simpler approximate expression of the high Q behavior of the single chain dynamics can be obtained:

$$\frac{I_{chain}(Q,t)}{S_{chain}(Q)} = \int_0^\infty exp\left\{-u - \frac{2}{\pi}\sqrt{\Omega_R t}\left[\sqrt{\pi}e^{\frac{u^2}{4\Omega_R t}} + \frac{1}{2}\pi\frac{u}{\sqrt{\Omega_R t}}\left(1 - Erf\left(\frac{u}{2\sqrt{\Omega_R t}}\right)\right)\right]\right\} \quad (17a)$$

The only variable in Eq. (17a) is $\Omega_R t = \frac{Wl^4}{36}Q^4 t$, which allows to construct a master curve of data taken at different Q values. We are going to use this model to calculate the Rouse time, t_R, and calculate the elementary Rouse rate W in the hands-on-experiment.

2.3. Reptation dynamics

As the polymers length increases above the entanglement molecular weight (M_e), the available conformations are limited by additional topological constraint which can be thought of as 'reptation tube' as illustrated in Figure 7. The polymer chain then starts to move along the tube, which is called reptation.

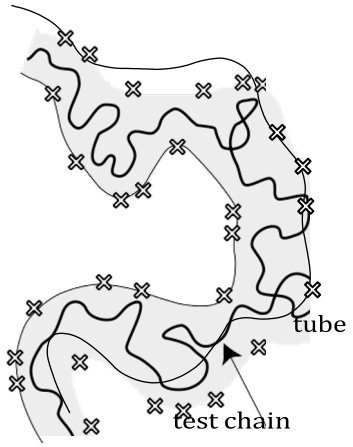

Figure 7. Illustration of the reptation tube. The test chain is trapped in a tube (indicated by the gray area) created by neighboring chains. The crossings represent the intersection of the neighboring chains with the curved surface on which the test chain lies. The test chain moves along the tube like a reptile, whose motion is called reptation motion (adapted from [8]).

Accordingly, the single chain ISF will change. Qualitatively we would expect to measure the following behavior with increasing time, illustrated in Figure 8:

i. At short times, the chain will perform unrestricted Rouse motion.

ii. In the regime of local reptation the chain has already explored the tube laterally and further density fluctuations of the labelled chain will only be possible via Rouse relaxation along the tube. Under such circumstances the structure factor, to a first approximation, will mirror the form factor of the tube $I_{chain}(Q,t)/I_{chain}(Q) \approx \exp(-Q^2d^2/36)$. In this regime the experiment should reveal the size of the topological constraints, *i.e*. the reptation tube diameter, d, without applying any detailed model.

iii. In the creep regime, $t > t_R$ the memory of the tube confinement will be gradually lost.

iv. Finally, at even longer times at very small Q (QR_g<<1), the reptation diffusion will be probed.

A tractable analytic expression for the coherent dynamic structure factor in the regime ii can be obtained by neglecting the initial Rouse regime. Thus, the dynamic structure factor is composed from two contributions $I^{loc}(Q,t)$ and $I^{esc}(Q,t)$ reflecting local reptation and escape processes (creep motion) from the tube:

$$\frac{I_{chain}(Q,t)}{I_{chain}(Q)} = \left[1 - exp\left(-\frac{Q^2d^2}{36}\right)\right] I^{loc}(Q,t) + exp\left(-\frac{Q^2d^2}{36}\right) I^{esc}(Q,t) \qquad (18)$$

The local reptation part is:

$$I^{loc}(Q,t) = exp\left(\frac{t}{\tau_0}\right) erfc\left(\sqrt{\frac{t}{\tau_0}}\right) \qquad (19)$$

Where $\tau_0 = \frac{36}{Wl^4Q^4}$ and *erfc* is the complementary error function. In the NSE timescale, it is sufficient to assume $I^{esc}(Q,t)$=1, because the creep motion is too slow. A pronounced plateau in $I_{chain}(Q,t)$ is a signature for confined motion. In the hands-on-experiment, we will access the tube diameter d from the Q-dependent plateau with this reptation model, Eq. (18).

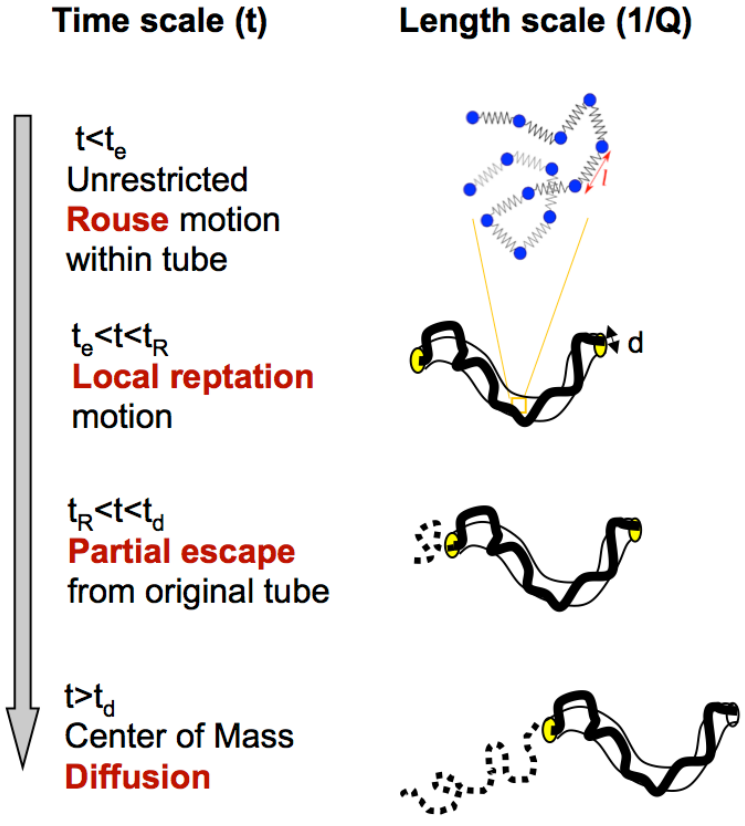

Figure 8. The regimes of an entangled chain dynamics. t_e is the cross-over time from Rouse to reptation behavior; t_R is the Rouse time; t_d is the terminal time after which the chain has left its original tube.

3. Hands-on-Experiment: Rouse dynamics and reptation tube in Poly(Ethylene Oxide) melts

3.1 Sample characteristics

The polymer used in the experiments is poly (ethylene oxide) (PEO). The repeating unit of PEO is ethylene glycol and the end groups are typically -OH as shown in Figure 9.

PEO is hydrophilic, biocompatible and easy to crosslink to form gels with tunable mechanical properties suitable for many biomedical applications such as drug release. [10] In addition, PEO is one of the most widely studied polymers for ion conducting membranes in lithium-ion batteries due its ability to form complexes with a variety of salts. [11] The glass transition temperature of PEO is $T_g \approx 213$ K. Due to the lack of bulky groups on the chain backbone, PEO crystallizes below $T_m \approx 340$ K to adopt a semi-crystalline phase (coexisting mixture of amorphous and crystalline phases). The entanglement molecular weight of PEO is $M_e \approx 2$ kg/mol. Some other physical parameters for the homopolymer we will use are listed in Table 2.

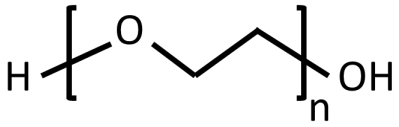

Figure 9. Molecular structure of linear polyethylene oxide with OH terminated ends.

Table 2. The physical parameters for PEO used in NSE experiments

Properties	**Deuterated *PEO***	**Hydrogenated *PEO***
Formula	$(C_2D_4O)_n$	$(C_2H_4O)_n$
M_W/ g mol^{-1}	35,000	35,000
Dispersity	1.09	1.08
Density/ g ml^{-1}	1.06	1.06
SLD/ Å^{-2}	6.08×10^{-6}	0.6×10^{-6}

3.2 Planning the NSE experiment

A successful experiment in NSE requires careful planning of the sample preparation as well as of the measurements.

3.2.1. Setting the goal

The large scale dynamical properties of a given long linear polymer can be estimated by knowing the elementary Rouse parameter, Wl^4, and the reptation tube diameter, d. Both Wl^4 and d can be determined for PEO using NSE at an appropriate temperature. We will perform NSE experiments in the liquid state of PEO at 400 K, well-above the melting point and where PEO has been studied in NSE previously. [11-13]

Q2. In NSE, we measure the dynamic structure factor up to 100 ns. What types of chain motions would you expect to observe for PEO with Mw=300 Da, Mw=2 kDa, and Mw=35 kDa at 400 K in NSE? What about PolyStyrene, Mw=100kDa?

3.2.2. Obtain the single-chain conformation

The contrast from the single chain is obtained by homogenously mixing a small amount of hydrogenated polymer in a matrix of deuterated polymer of the same molecular weight. This way the incoherent scattering from the hydrogenated chains is minimized while sufficiently large amount of scatterers are introduced in the material. Typically, 10 % to 25 % hydrogenated chains are used. In this experiment, we will use 25 % h-PEO in 75 % d-PEO of M_w=35 kg/mol (supplied by Polymer Source Inc.[*]). In such conditions, the SANS profiles from the single chain PEO was obtained as shown in Figure 10.

Q3. Calculate the contrast between h-PEO and d-PEO. Consider the following mixtures of h-PEO and d-PEO: 10 % h-PEO/90 % d-PEO, 20 % h-PEO/80 % d-PEO, 50 % h-PEO/50 % d-PEO, 90 % h-PEO/10 % d-PEO; what advantages and disadvantages do each of these compositions offer for a NSE experiment? Imagine to disperse gold nanoparticles in your PEO polymer matrix, how could you contrast match the nanoparticles?

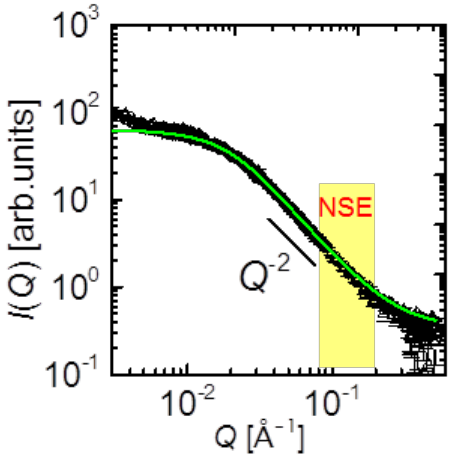

Figure 10. SANS profile obtained from 35 kg/mol PEO (25/75 h-PEO/d-PEO). [13] The line is the best fit to Debye form factor, $f_{\text{Debye}}(Q^2R_g^2)$, [Eq. 12] for a Gaussian chain with $R_g \approx 7$ nm.

3.2.3. Determine the time and length-scales of interest

This is perhaps the most important step in the experimental planning. Here, we should consider both sample behavior and instrument limitations to optimize the measurements.

Our goal is to obtain the intermediate scattering function, ISF, and determine the elementary Rouse parameter, W, as well as the length of the confining tube along which the chains

[*] The identification of any commercial product or trade name does not imply endorsement or recommendation by the National Institute of Standards and Technology.

reptate, d. Therefore, we want to be at $Q<<2\pi/l$, with l being the segment length, to observe the segmental level relaxation. For PEO, l=5.8 Å, so you want to choose, $Q<<$ 1 Å^{-1}. However, this should not be our highest limit. We want to measure the collective dynamics which requires the signal to be from coherent scattering as opposed to incoherent scattering (that would give the self-motion of H-atoms often measured in HFBS). If we look at the SANS profile in Figure 10, the incoherent background starts contributing significantly above (0.2 to 0.3) Å^{-1}. To avoid further difficulties on subtracting the incoherent scattering, we will limit the highest Q to be 0.3 Å^{-1}.

At larger length scales, if $Q < 2\pi/R_E$ (≈0.05 Å^{-1} for PEO), we probe the whole chain and may observe the creep motion (for long entangling chains) or center of mass diffusion (for short unentangling chains) in addition to internal Rouse modes (this also strongly depends on the timescale of the technique as discussed next). So, the nature of the sample itself narrows down our length-scale of interest to the range 0.05 Å^{-1} < Q <0.3 Å^{-1}.

We now determine the dynamic range. Again, we want to see both the Rouse decay and entanglement plateau, so we need to estimate the crossover time between the two regimes, t_e. From the literature, $t_e \approx$ 10 ns for PEO at 400 K, [12] which sets the lower limit for the longest Fourier time to be measured.

To summarize, our measurements should be performed at 0.05 Å^{-1} < Q <0.3 Å^{-1} and $t_{NSE,max}$ >>10 ns to achieve our goal.

Q4. How would you estimate the crossover time between Rouse and entanglement if you never directly measured in NSE before?

3.2.4 Determine the instrument configuration

For the accessible Q-range and dynamics range of NSE, refer to the table given below (https://www.ncnr.nist.gov/instruments/nse/NSE_details.html)

NSE Instrument Details

Guide	NG-A, 50 mm (width) 70 mm (height)
λ	from 4.5 Å to 12 Å, Δλ/λ 20 %
Flux at Sample Position	3.1×10^7 neutrons/cm^2/s at 5 Å
	2.7×10^7 neutrons/cm^2/s at 6 Å
	1.3×10^7 neutrons/cm^2/s at 8 Å
	5.0×10^6 neutrons/cm^2/s at 11 Å
	1.4×10^6 neutrons/cm^2/s at 15 Å
Maximum field integral	0.44 T·m
Typical sample size	3 cm × 3 cm
Accessible scattering angle range	from 2° to 105°
Accessible *Q* range	from 0.060 Å^{-1} to ≈1.80 Å^{-1} at λ = 5 Å
	from 0.050 Å^{-1} to ≈1.50 Å^{-1} at λ = 6 Å
	from 0.035 Å^{-1} to ≈1.10 Å^{-1} at λ = 8 Å
	from 0.025 Å^{-1} to ≈0.80 Å^{-1} at λ = 11 Å
	from 0.020 Å^{-1} to ≈0.60 Å^{-1} at λ = 15 Å
Maximum field integral	0.44 T·m
Dynamic range	from 3 ps to 10 ns at λ = 5 Å
	from 5 ps to 15 ns at λ = 6 Å
	from 10 ps to 40 ns at λ = 8 Å
	from 50 ps to 100 ns at λ = 11 Å
	from 150 ps to 200 ns at λ = 15 Å
Detector	32 cm × 32 cm PSD

We now want to determine the wavelength to be used based on our Q and dynamic range of interest. Apparently, the Q-range we are interested in ($0.05\ Å^{-1} < Q < 0.3\ Å^{-1}$) can be accessed using λ = (6, 8, 11 and 15) Å. For the dynamic range, we would like to obtain times well above the crossover time, $t_{NSE,max} >> 10$ ns. 15 ns (at λ = 6 Å) and 40 ns (at λ = 8 Å) may not be enough to identify the entanglement plateau. Therefore, using λ = 11 Å which gives Fourier times up to 100 ns would be ideal.

Q5.λ = 15 Å can allow Fourier times up to 200 ns. What is the main limitation of using this configuration, particularly for our polymer sample?

In summary, we will perform our experiments using the following configuration:
Neutron wavelength: *11 Å*
Fourier times: *(0.5, 1, 2, 5, 8, 10, 20, 30, 50, 65, 80, 90, 95 and 100)* ns
Q-range: $0.05\ Å^{-1} < Q < 0.3\ Å^{-1}$
Temperature: *400 K*

3.2.5 Resolution, transmission and background

We will use charcoal as a resolution and fully deuterated PEO as the background. We obtain the echoes at the same configurations as used for the sample. The transmission for the sample and background will be measured and used for background subtraction. See Appendix A for the detailed procedure.

3.3 Data interpretation

NSE experiment measures the single chain dynamics of the PEO molecules. The data for $t < t_e$ will be analyzed using Eq. (17a) and compared with the results reported in the literature. [12] Similarly the data for $t > t_e$ will be globally fitted for all Q using Eq. (18) fixing the value of τ_0 to its reported value. [12]

Compare the results obtained with those reported in Table 3, and, please, fill in the missing values for the structural and dynamical properties of PEO at 400 K.

Table 3. The static and dynamic chain parameters for 35 kg/mol PEO at 400 K.

Parameters	Definition	Value	Unit
Segment length	l	0.58	nm
Rouse parameter	Wl^4	1.51	nm^4/ns
End-to-end distance	Nl^2		nm^2
Tube diameter	d		nm
Molar mass of monomer	M_o	44	g/mol
Total number of segments	N		-
Entanglements per chain	M_w/M_e		-
End-to-end distance	$R_E = \sqrt{Nl^2}$		nm
Radius of gyration	$R_g = \sqrt{Nl^2/6}$		nm
Rouse diffusion coefficient	$D_R = Wl^4/(3R_E^2)$		nm^2 /ns
Rouse time	$t_R = N^2/(\pi^2 W)$		ns
Crossover time between Rouse and Reptation	$t_e = \frac{d^4}{\pi^2 W l^4}$		ns
Reptation time	$t_d = \frac{3N^3}{\pi^2 W}\left(\frac{l}{d}\right)^2$		ns
Reptation diffusion coefficient	$D_{Rep} = \frac{R_g^2}{\tau_d}$		nm^2 /ns

NSE results provide microscopic information on the parameters of the Rouse dynamics as well as on the tube size of PEO. These parameters can also be determined from macroscopic measurements of the polymer's rheology. The monomeric friction coefficient is a basic quantity in all rheological measurements. This quantity can be inferred indirectly for example from viscosity measurements, where in the Rouse regime, i.e. for molecular weight below entanglement:

$$\eta^{Rouse} = \frac{N_A}{36}\frac{\rho}{M_0}\zeta l_{mon}^2 N_{mon} \quad (20)$$

Where N_A is the Avogadro number, ρ is the polymer density, M_0 is the monomer mass, $l_{mon}^2 = \frac{R_E^2}{M} M_0$, and $N_{mon}=N/n$, n being the number of bonds per monomer. The monomeric friction coefficient ζ is directly related to the Rouse rates which can be obtained from the dynamic neutron scattering measurements:

$$\zeta = \left(\frac{3k_BT}{Wl^4}\right) l_{mon}^2 \quad (21)$$

For molecular weights above entanglement:

$$\eta^{Reptation} = q\eta^{Rouse}\left(\frac{M}{M_e}\right)^2 \quad (20)$$

Where q is a prefactor which in this case can be approximated to 1.[12]

The dynamic modulus of a polymer melt is characterized by a plateau in frequency which broadens with increasing chain length. In this plateau regime, the polymer melt acts like a rubber. In analogy, it is suggestive to assume that the entanglements between the chains in a melt lead to the formation of a temporary network, which then displays rubber elastic properties. Based on such assumptions, the reptation model of de Gennes [4] and Doi and Edwards [14] was formulated. In this model, the dominating chain motion is a reptile-like creep along the chain profile, the reptation tube. *d* relates to the plateau modulus of the melt as:

$$d^2 = \frac{4}{5}\frac{R_E^2}{M}\rho N_A \frac{k_BT}{G_N^0} \quad (22)$$

with G_N^0, being the plateau modulus.

Using the Eqs. (20) to (22), compare the predictions of the rheological theories on the basis of the NSE results with the values reported in the literature [12,15] for the viscosity and plateau modulus of PEO.

Reference:

[1] F. Mezei, *Z. Physik*. **255**, 146 (1972).

[2] F. Mezei, in *Lecture Notes in Physics* **128**, (1980).

[3] D. Richter, M. Monkenbusch, A. Arbe, and J. Colmenero, *Adv. Polym Sci*. **174**, 1 (2005).

[4] P. G. de Gennes *J. Chem. Phys.* **55**, 572 (1971).

[5] P. Schleger B. Farago, C. Lartigue A. Kollmar, and D. Richter, *Phys. Rev. Lett.* **81**, 124 (1998).

[6] P. J. Flory Principles of polymer chemistry. Cornell University Press, London (1953).

[7] P. R. Rouse *J. Chem. Phys.* **21**, 1272 (1953).

[8] I. Teraoka, in Polymer Solutions: An Introduction to Physical Properties, A John Wiley & Sons, Inc. (2002).

[9] H. Montes, M. Monkenbusch, L. Willner, S. Rathgeber, L. J. Fetters, and D. Richter, *J. Chem. Phys.* **110**, 10188 (1999).

[10] F. M. Veronese and G. Pasut, *Drug discovery today* **10**, 1451 (2005).

[11] C. Do, P. Lunkenheimer, D. Diddens, M. Götz, M. Weiß, A. Loidl, X.-G. Sun, J. Allgaier, and M. Ohl, *Physical Review Letters* **111**, 018301 (2013).

[12] K. Niedzwiedz, A. Wischnewski, W. Pyckhout-Hintzen, J. Allgaier, D. Richter, and A. Faraone, *Macromolecules* **41**, 4866 (2008).

[13] E Senses, S.M. Ansar, C.L. Kitchens, Y. Mao, S. Narayanan, B. Natarajan, and A. Faraone, *Phys. Rev. Lett.* **118**, 147801 (2017).

[14] M. Doi and S. F. Edwards, *J. Chem. Soc. Farad Trans.* **274**, 1789 (1978); ibid. **274**, 1789 (1978); ibid. **275**, 38 (1978).

[15] L. J. Fetters, D. J. Lohse, and W. W. Graessley, *J. Polym. Sci. Part B; Polym. Phys.* **37**, 1023 (1999).

Further Readings:

Neutron spin echo

- Edited by F. Mezei, Lecture Notes in Physics 128, Neutron Spin Echo, Springer-Verlag (1980).
- Edited by F. Mezei, C. Pappas, T. Gutberlet, Lecture Notes in Physics 601, Neutron Spin Echo Spectroscopy, Springer-Verlag (2003).

General neutron scattering

- G.L. Squires, in Introduction to the theory of thermal neutron scattering, Dover Publications, Inc. (1978).
- Edited by T. Imae, T. Kanaya, M. Furusaka, N. Torikai, Neutrons in Soft Matter, Wiley (2011).

Polymer structure and dynamics

- B. Ewen and D. Richter, Advances in Polymer Science **134**, 1-130 (1997).
- I. Teraoka, in Polymer Solutions: An Introduction to Physical Properties, A John Wiley & Sons, Inc. (2002).
- D. Richter, M. Monkenbusch, A. Arbe and J. Colmenero in Advances in Polymer Science **174**, 1-221 (2005).

Appendix A:
The principle of neutron spin echo

A.1. The NSE technique and the spectrometer

Figure 3 in the main text shows in detail the manipulation of the neutron spins through the NSE spectrometer. After the neutron beam ($\Delta\lambda/\lambda$ = 10% to 20%, depending on the tilt angle of the velocity selector) is polarized in the longitudinal direction by a Mezei cavity, the neutron spins are rotated by 90° by the first π/2-flipper, which begins the precession of the neutron in the field produced by the main coil. In a perpendicular magnetic field H_1, a neutron spin will undergo precessions at a frequency $\omega_L = -\gamma_L H_1$. If a neutron is polarized perpendicular to a homogeneous field, it will precess through an angle

$$\varphi_i = \gamma_L \frac{m_n \lambda}{h} \int_i H_i(l) dl = \gamma_L \frac{m_n \lambda}{h} J_i \qquad \text{(A1)}$$

where $J_i = \int_i H_i(l) dl$ is the field integral along solenoid i. Note that the maximum J_i for the NGA-NSE is ≈ 0.5 Tm. For a beam of neutrons with an incident wavelength distribution $f(\lambda)$ and $\langle\lambda\rangle = \langle\lambda_1\rangle$, each neutron undergoes a spin precession of $\phi_1(\lambda)$ in the first arm of the spectrometer. The neutron beam, with its broad band of wavelength, will completely depolarize in this first precession field. Just before scattering from the sample, a neutron passing through the π-flipper will change its phase from $\phi\ (mod\ 2\pi)$ to $-[\phi\ (mod\ 2\pi)]$. Then, on passing through the second precession field, if the scattering is elastic and the two field integrals are the same, the beam recovers its full polarization at the second π/2-flipper, which rotates the spins back to the longitudinal direction, thereby stopping the precessions.

If the neutrons are scattered quasi-elastically from the sample, changing wavelength by $\delta\lambda$, then they will undergo a spin precession with phase angle ϕ_2 in the second arm of the spectrometer. The phase difference will be:

$$\varphi = \phi_1(\lambda) - \phi_2(\lambda + \delta\lambda) = \phi_1(\lambda) - \phi_1(\lambda + \delta\lambda) + \Delta\phi(\lambda + \delta\lambda) \qquad \text{(A2)}$$

where $\Delta\phi(\lambda) = \phi_1(\lambda) - \phi_2(\lambda)$.

To the first order in $\lambda\delta\lambda$ and $\Delta\phi$, the phase shift is composed of a term from the inelasticity and a term from the difference in the field integrals (recall that $\phi \propto \lambda$):

$$\varphi = \phi_1(\langle\lambda_1\rangle)\frac{\lambda}{\langle\lambda_1\rangle} - \phi_1(\langle\lambda_1\rangle)\frac{\lambda+\delta\lambda}{\langle\lambda_1\rangle} + \Delta\phi(\langle\lambda_1\rangle)\frac{\lambda}{\langle\lambda_1\rangle} = \frac{\phi_1(\langle\lambda_1\rangle)\delta\lambda + \Delta\phi(\langle\lambda_1\rangle)\lambda}{\langle\lambda_1\rangle} \qquad \text{(A3)}$$

The inelasticity of the scattering can be written as a change in wavelength:

$$\hbar\omega = \Delta E = E_1 - E_2 = \frac{h^2}{2m_n}\left[\frac{1}{\lambda^2} - \frac{1}{(\lambda+\delta\lambda)^2}\right] \qquad \text{(A4)}$$

where to the first order in $\delta\lambda$

$$\hbar\omega = \frac{h^2}{m_n}\frac{\delta\lambda}{\lambda^3} \qquad \text{(A5)}$$

which connects $\delta\lambda$ to ω (or equivalently to ΔE; please, keep also in mind that it is common practice to indicate ΔE simply as E).

Due to the quantum nature of the neutron spin, only one component of the spin, call it *z*, can be determined. The polarization of the scattered beam, which is the quantity measured during a NSE experiment, is given by:

$$\langle P_z \rangle = \langle \cos(\varphi) \rangle = \int f(\lambda)\, d\lambda \int S(Q,\omega) \cos\left[\frac{\phi_1(\langle\lambda_1\rangle)\frac{m_n\lambda^3}{2\pi h}\omega + \Delta\phi(\langle\lambda_1\rangle)\lambda}{\langle\lambda_1\rangle}\right] d\omega \quad \text{(A6)}$$

where we have integrated over the distribution of incoming wavelength and exchanged energies, this latter distribution being defined by the scattering function $S(Q,\omega)$.

Since we have assumed $S(Q,\omega)$ is a quasi-elastic scattering law, which is essentially an even function of ω, the cosine can be factorized:

$$\begin{aligned}\langle P_z \rangle &= \int f(\lambda) \cos\left[\frac{\Delta\phi(\langle\lambda_1\rangle)\lambda}{\langle\lambda_1\rangle}\right] d\lambda \int S(Q,\omega) \cos\left[\frac{\phi_1(\langle\lambda_1\rangle)\frac{m_n\lambda^3}{2\pi h}\omega}{\langle\lambda_1\rangle}\right] d\omega \\ &= \int f(\lambda) \cos\left[\frac{\Delta\phi(\langle\lambda_1\rangle)\lambda}{\langle\lambda_1\rangle}\right] d\lambda \int S(Q,\omega) \cos(\omega t_F)\, d\omega \end{aligned} \quad \text{(A7)}$$

where

$$t_F = \frac{\phi_1(\langle\lambda_1\rangle) m_n \lambda^3}{2\pi h \langle\lambda_1\rangle} = \gamma_L \left(\frac{m_n}{h}\right)^2 \frac{\lambda^3}{2\pi} J_i \quad \text{(A8)}$$

is the Fourier time.

Q6. In practice, how do we get longer Fourier times?

Q7. How many turns of neutron spins do you expect? Compare different Fourier time conditions.

By adjusting the field so that the echo condition is met (J_1=J_2, *i.e.*, $\Delta\phi$=0), the beam polarization is:

$$\langle P_z \rangle = \int f(\lambda)\, d\lambda \int S(Q,\omega) \cos(\omega t_F)\, d\omega = I(Q,t_F) \quad \text{(A9)}$$

$I(Q,t)$ is the intermediate scattering function (ISF), which is the spatial Fourier transform of the van-Hove correlation function $G(r,t)$ (remember that $G(r,t)$, classically, represents the probability that given a particle at the origin at time zero, a particle is at position *r* at time *t*. *G* is composed of a self, $G_s(r,t)$ probed by incoherent scattering, and of a distinct part). The scattering function $S(Q,E)$ is the cosine transform of $I(Q,t)$. In many experimental cases $I(Q,t)$ varies slowly with λ, and so it can be removed from the integrand. In these cases, NSE spectroscopy directly measures the ISF and it is not necessary to determine the wavelength distribution.

The notion "high resolution" used in connection with NSE instruments means high achievable Fourier times, t_F. There are two parameters available to influence t_F: the neutron wavelength λ and the field integral *J*. The former depends on the neutron source characteristics as well as on the desired *Q*-range. At the NCNR the highest neutron flux is at λ ≈ 6 Å, and in order

to reach higher t_F a price in terms of the neutron flux has to be paid. The field integral depends on the design and characteristics of the spectrometers. Different issues limit its value. Achieving a high value of J by aiming at a value of the magnetic field H is limited by the costs and by the unavoidable inhomogeneity of J, *i.e.* the differences of J along different neutron paths have to be small compared to the value corresponding to half a precession. In order to reduce the inhomogeneities related to the radial variation of the field and to the different path length present in a divergent beam, special correcting elements, the so-called "Fresnel coils", have to be inserted along the flight path. Figure A1 shows the resolution of the NCNR NSE spectrometer at different wavelengths.

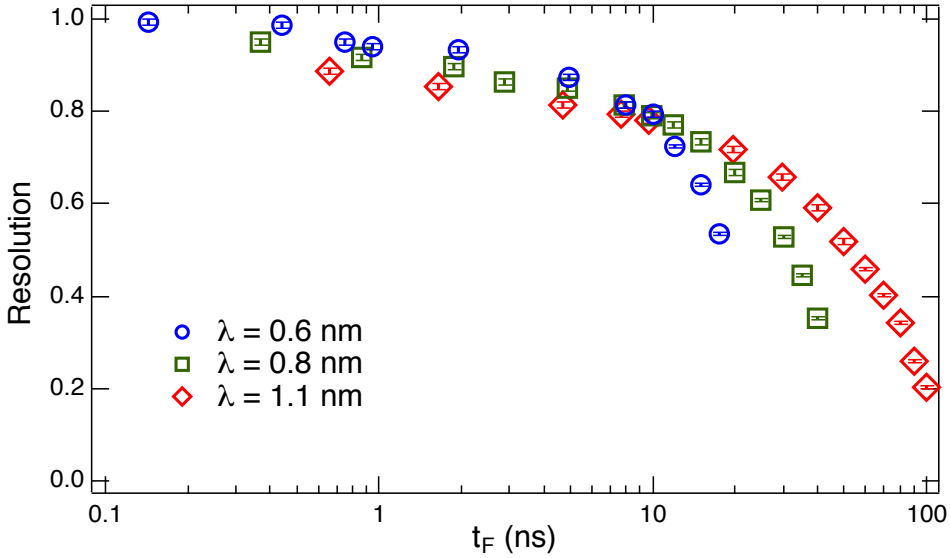

Figure A1. Wavelength dependence of the resolution function.

The polarization of the scattered neutrons at the end of the second precession field is detected by an analyzer, made of an array of supermirrors in front of the detector that transmits only neutrons of one polarization direction. Neutrons are detected by a 32×32 cm^2 multidetector with a resolution of 1 cm^2. We will see in the data reduction section how to take full advantage of the multidetector to measure different Q values at the same time.

A spin echo measurement is usually performed by setting the spectrometer to the echo condition (J_1=J_2), obtaining the ISF using Eq. (A10). As shown in Fig. 5, in practice the counting rate (N) is measured for several phase current (ϕ_c) values near the echo position, then fitted to a Gaussian damped cosine function to give the echo amplitude, A:

$$N = N_0 + A exp\left[\frac{(\phi_c-\phi_0)^2}{2\sigma^2}\right] \cos\left[\frac{360}{T}(\phi_c - \phi_0)\right] \qquad \text{(A10)}$$

Q8.Can you explain why Eq. (A10) is used to fit the echo?

Q9. What is the relation between the fitting parameters σ and T and the incoming wavelength distribution $f(\lambda)$?

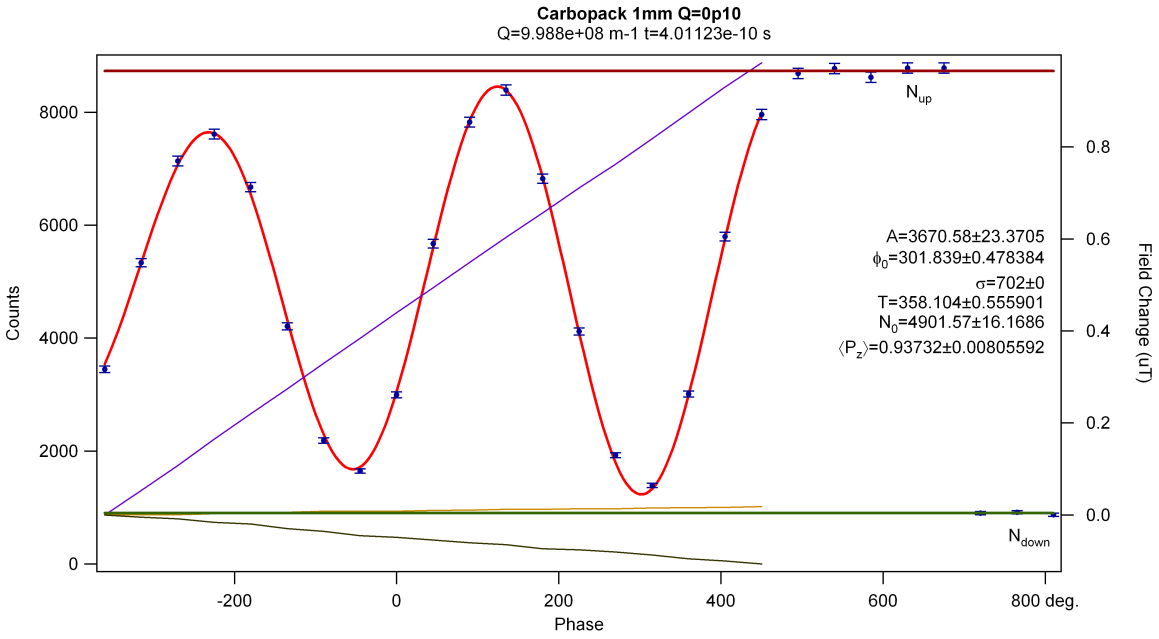

Figure A2. NSE signal as a function of the phase difference between the incident and scattered beams. The red curve is the fit according to Eq. (A10) (can you tell why σ is a fix parameter?). The blue, orange, and black lines are the magnetic field along the three orthogonal directions at the sample position. In this way the presence of stray magnetic fields due to the environment can be recorded.

The effect of the less-than-perfect efficiency of the flippers, the polarizer, and the analyzer is removed by measuring the count rates with the π/2-flippers off and the π-flipper both off and on, giving the non spin flip, N_{up}, and spin flip counts, N_{down}, respectively. The measured value of the polarization of the scattered beam at the echo point $\langle P_z \rangle_S$ is given by:

$$\langle P_z \rangle_S = \frac{2A}{N_{up} - N_{down}} \tag{A11}$$

Inhomogeneities in the magnetic field may further reduce the polarization. As these inhomogeneities are not correlated with $S(Q,\omega)$ or $f(\lambda)$, their effect may be divided out by measuring the polarization from a purely elastic scatterer:

$$\langle P_z \rangle_E = \frac{2A^E}{N_{up}^E - N_{down}^E} \tag{A12}$$

In order to ensure that the dynamic scattering from everything that is not our sample is accounted for, a background measurement must be performed. The sample holder (including the pure solvent, if any) must be measured under identical conditions as your sample.

The normalized ISF is then obtained by:

$$\frac{I(Q,t)}{I(Q,0)} = \left[\frac{2\left(A - T_r A^{bgr}\right)}{\left(N_{up} - N_{down}\right) - T_r\left(N_{up}^{bgr} - N_{down}^{bgr}\right)} \right] \Big/ \frac{2A^E}{N_{up}^E - N_{down}^E} \tag{A13}$$

where T_r is the ratio of the transmissions of the sample and the background sample. Therefore, transmissions of both the sample and the solvent (with respect to an empty beam) must be measured at the respective wavelength, so that the correct fraction of solvent scattering (echo amplitude) can be subtracted.

In an NSE experiment, only scattering in the direction of the second arm can be measured. However, using a multidetector, it is still possible to measure $I(Q,t)$ at different Q values (around the mean Q value, determined by the scattering angle). At the NSE spectrometer at the NCNR, the scattering angle can be varied between ≈2° and 105°. The time is varied, according to Eq. (A8), by changing the field in the main coils.

Having measured the scattering function in the time domain, from Eq. (A13) it can be seen that unlike other spectrometers, the instrumental resolution effects in NSE spectroscopy may be simply divided out by measuring the response of a purely elastic scattering sample. This is a great advantage and spares the user the often complicated task of deconvolving the instrumental energy lineshape from the physical lineshape from the sample.

Q10.	How do you know if your sample scatters "well" or "good enough"?
Q11.	How long do you have to count for each measurement?

A.2. Data reduction

NSE data reduction is not a straightforward process. This is mostly due to the fact that we want to achieve full benefit from the multidetector. In fact, the echo determination must be done patch by patch on the detector surface to account for the residual phase shifts observed. The pixels are usually binned into areas of 2×2 or 4×4 pixels, and then these areas are analyzed individually. This process must be performed very carefully especially for the resolution. It is important that the measured phase varies smoothly on the surface of the detector and that it varies about linearly for each area as a function of the time. This is not always easy, especially near the edge of the detector or at high Fourier times, where the signal-to-noise ratio is not very good. Luckily, once the phases are determined for the resolution they can be 'imported' for the analysis of the sample itself and of the background.

Finally, data from areas (usually ring segments) representing the same momentum transfer Q are collected and evaluated into several $I(Q_i,t)/I(Q_i)$ curves. For this reason we have to accurately measure the position of the beam center.

Q12.	Each pixel of the 2-D detector counts neutrons with a slightly different efficiency (± 10 %). Does the non-uniformity of the detector need to be accounted for?

Appendix B:
Incoherent scattering measurements with NSE spectroscopy from Hydrogenous Samples

There are three sources of incoherent scattering: isotopic variation in the nuclear cross-section, uncorrelated motions, and variation in the nuclear cross section due to the nuclear spin. In this appendix, we discuss nuclear spin incoherence, specifically as it is applied to hydrogenated samples.

With the classical NSE spectrometer design, it is possible to measure the nuclear incoherent intermediate structure factor $I_{incoh}(Q,t)$ in addition to the coherent intermediate structure factor discussed above [$I_{coh}(Q,t)$]; however, in practice, some difficulties need to be overcome. Most importantly, the incoherent scattering intensity is often low. The incoherent scattering is spread out isotropically in a solid angle of 4π, therefore its intensity is generally much lower than the intensity of coherent scattering, which is concentrated in a limited region of the Q space (consider for example how the SANS signal compares to the incoherent background).

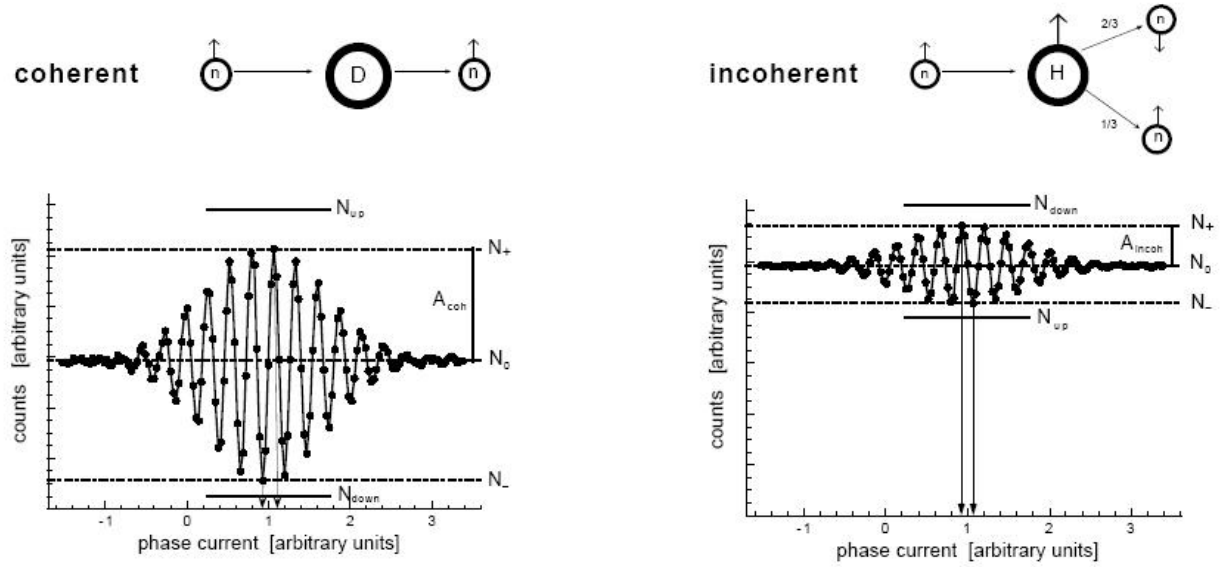

Figure B1. NSE signal as a function of the phase difference between the incident and scattered beams. The upper part of the figures shows the principle difference, in the case of deuterons and protons, between the scattering from a nucleus with and without nuclear spin. The lower part shows the NSE signals obtained in both cases – the count rate is plotted against the current of the phase correction coil. A_{coh} and A_{incoh} are the echo amplitudes for coherent and incoherent scattering, N_0 is the average count rate outside the echo, N_+ and N_- are the maximal and minimal count rates with the π/2-flippers on, and N_{NSF} and N_{SF} are the count rates of non spin flip (π-flipper off) and spin flip (π-flipper on) measurements made with the π/2-flippers off.

Moreover, the nuclear spin incoherent scattering intrinsically reduces the polarization of the scattered beam, and therefore the echo amplitude, as shown in Fig. B1. Nuclear spin incoherence causes, with a nucleus dependent probability, a spin flip of both the inelastically and elastically scattered neutrons. For example, 2/3 of the neutrons scattered from an H atom undergo a spin flip, whereas deuterium, which has no nuclear spin, has no influence on the neutron spin. In nuclear spin incoherent scattering processes, some fraction of the neutron spins are flipped by 180° and produce an echo that is reversed with respect to the non-spin-incoherent case. The overall echo amplitude is a superposition of the signals with opposite sign from the spin-flipped and non-spin-flipped neutrons, and so is reduced. For scattering from H atoms, the final signal is -1/3 of the signal from the non-spin-incoherent scattering case; the background is strongly increased as well, reducing the signal-to-noise ratio considerably. In the ideal case a purely incoherent scatterer gives a flipping ratio (N_{NSF}/N_{SF}) of 0.5, whereas for coherent scattering flipping ratios of the order of ten are customary. If, in addition, there is some coherent scattering present, the spin incoherent and coherent cross sections have opposite signs for the echo signal and so reduce the echo signal in a way that cannot be decomposed.

However, if the incoherent signal is strong enough, for example in the case of aqueous systems, the incoherent scattering can be measured. With respect to a measurement performed with a time-of-flight or a backscattering spectrometer, the main benefits are a better energy resolution and the advantage of working in the time domain. The main drawback is that each Q value has to be measured separately. In any case, long counting times are to be expected.

For these reasons, the main application of NSE spectroscopy is still to measure the coherent intermediate scattering function $I_{coh}(Q,t)$, the coherent density fluctuations that correspond to the SANS intensity pattern. The coherent scattering may be orders of magnitude more intense than the incoherent contributions. However, studies of the incoherent dynamics with NSE are possible and in some cases have been successfully performed in the past.

Appendix C:
Magnetic scattering measurements with NSE spectroscopy

You now know that the neutron spin echo technique is the neutron scattering method with the highest energy resolution. Relaxation times of several nanoseconds (corresponding to a resolution of the order of 100 neV) are easily measured and hence the technique is suited for slow dynamics. Although the majority of experiments done on a NSE spectrometer involve soft condensed matter, the technique is also very important in the study of magnetic samples with slow spin dynamics. By utilizing polarized neutrons, NSE allows the separation of magnetic and nuclear coherent and incoherent scattering.

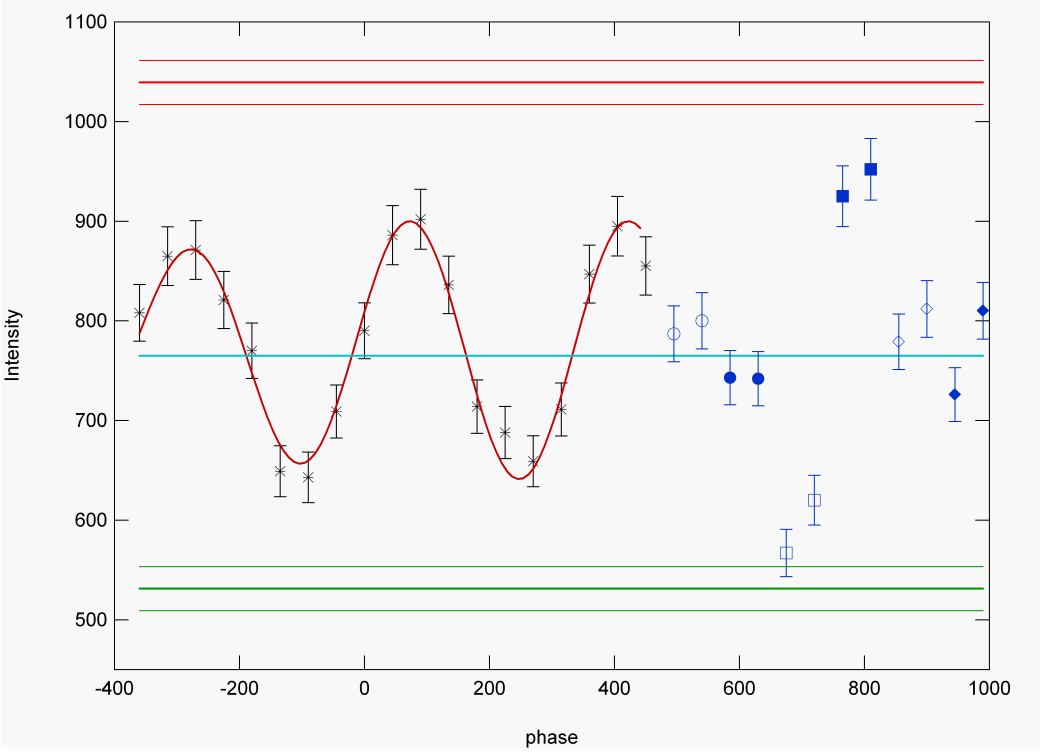

Figure C1. Example of an echo measured for a magnetic signal. The last six points are the measurement of the xyz polarization. The open symbols refer to the down measurements (no spin inversion) and the closed symbols to the up measurements (spin inversion). x: circles; z: squares; y: diamonds. Note the 'inversion' for the z measurements: the up counts are much higher than the down. In fact, the magnetic intensity is: $S^M(Q)=2(z_{up}-z_{dwn})-(x_{up}-x_{dwn})-(y_{up}-y_{dwn})$. The cyan line represents the average intensity: $S(Q)=(z_{up}+z_{dwn}+y_{up}+y_{dwn}+x_{up}+x_{dwn})/6$. The distance between the red and green line is the normalization factor for the magnetic echo and is equal to the magnetic intensity divided by 2.

In fact, in NSE experiments with magnetic samples one almost always employs three-directional neutron polarization analysis (often referred to as *xyz* polarization analysis) to measure

the magnetic part of the static structure factor *S(Q)*. To do this the instrument is run in polarized diffraction mode without an echo but with a π flipper. One measures six cross sections with the magnetic field along three axes *x, y*, and *z* ('up' and 'down' for each).

Certain linear combinations of these cross sections cancel the nuclear coherent and incoherent scattering contributions, thus allowing the separation of the purely magnetic scattering, magnetic $S^M(Q)$. With polarized neutrons, one always identifies the magnetic scattering unambiguously.

During the echo experiment one takes advantage of the fact that a magnetic species does a π flip of the neutron (spin inversion). Therefore, one important difference between a magnetic experiment and the other experiments done on the spectrometer is the absence of the π flipper near the sample position. Now only the spin flipped neutrons from the magnetic scattering contribute to the echo, while the nuclear scattering generates a depolarized background. The remaining experimental details are the same. The echo amplitude, which is purely due to magnetic scattering, is then normalized to the magnetic $S^M(Q)$ obtained from the *xyz* polarization analysis.

The difficulties with magnetic NSE experiments include the weak signal, neutron depolarization from ferromagnetic components to the spin-correlations and the necessity for slow spin dynamics. The technique has however proven indispensable in spin-glass physics and frustrated magnetism.

NSE at a glance

- Sensitive to the time-dependent density-density correlation function. Directly measures the intermediate scattering function $I(Q,t)$.
- Bridges the gap in time scale between conventional inelastic neutron scattering and dynamic light scattering. (Q-range of 0.01–1.6Å $^{-1}$ and Fourier times of up to 10^{-7} s available.)
- NIST spectrometer is optimized for measurements of soft condensed matter systems. For example:

  Polymers
  Observation and quantitative description of the crossover in dynamics from local segmental diffusion to time-dependent behavior governed by entanglements occurring over longer length scales.
  Glassy dynamics
  Identification in polymer glasses of the intra- and inter- molecular dynamics responsible for the α and β_{slow} relaxation.
  Biological model systems
  Quantitative description of the effect of interlayer coupling in the extended diffusive mode of lipid bilayers.
  Proteins
  Intra-molecular diffusion in *e.g.,* pig immunoglobulin G.

- By using polarized neutrons, NSE provides an intrinsic separation of magnetic and nuclear scattering, making data analysis easy and the interpretation unambiguous for this kind of experiments.

Spectrometer Operating Characteristics

	Present	**Upgrade**
Scattering angle	up to 105°; Q_{max} = 1.25 Å^{-1} for 8Å.	up to 100°; Q_{max} = 1.20 Å^{-1} for 8Å.
Q_{min} and Q-resolution	<0.02Å^{-1}.	Same
Polarized beam for wavelengths:	> 4.7 Å.	Same
Maximum Field integral $\int\|B\|dl$ =	0.438 T·m (40 ns at 8Å).	≈1 T·m (100 ns at 8Å).
Flux (10% FWHM wavelength distribution).	2×10^6 n/cm^2/s at 8Å	× ≈2 (from cold source upgrade)
Typical sample size:	3×3 cm^2.	Same